

PHY407 Lab 3: Gaussian Quadrature and Numerical Differentiation

Work Distribution:

Emma Jarvis: Q1

Lisa Nasu-Yu: Q2, Q3

September 24, 2023

1 More on Integrating Functions

1.a

1.a.1

We started by evaluating the integral given by Eq. 1 using the Trapezoid rule, the Simpson's rule and the Gaussian Quadrature methods for a range of N slices/sample points from 8 to 2048. Table 1 summarizes the values obtained using these three methods.

$$I = \int_0^1 \frac{4}{1+x^2} dx \quad (1)$$

| N | Trapezoid Rule | Simpson's Rule | Gaussian Quadrature |
|------|--------------------|--------------------|---------------------|
| 8 | 3.138988494491089 | 3.1415925024587072 | 3.1415926535191185 |
| 16 | 3.140941612041389 | 3.1415926512248227 | 3.1415926535897896 |
| 32 | 3.141429893174975 | 3.141592653552836 | 3.1415926535897905 |
| 64 | 3.141551963485654 | 3.141592653589215 | 3.141592653589792 |
| 128 | 3.141582481063752 | 3.1415926535897847 | 3.141592653589793 |
| 256 | 3.1415901104582815 | 3.141592653589794 | 3.141592653589792 |
| 512 | 3.1415920178069214 | 3.141592653589787 | 3.1415926535897967 |
| 1024 | 3.141592494644072 | 3.1415926535897896 | 3.141592653589794 |
| 2048 | 3.1415926138533594 | 3.141592653589796 | 3.141592653589798 |

Table 1: Printed output values of Eq. 1 using three methods of integration; trapezoid, Simpson's and Gaussian quadrature for a range on N slices/sample points.

1.a.2

We then calculated the relative error of the three methods compared to the true value of 1, π , for each N value in Table 1. The relative error using the Gaussian quadrature method was computed using Eq. 2 by taking the difference between subsequent N values because each N value in that Table is double the previous value. Figure 1 depicts the relative errors using the Gaussian quadrature method, trapezoid rule and Simpson's rule. The plot is in log-log scale and shows that for each

value of N , the trapezoid method has the highest error, then the Simpson's rule has the second highest relative error for most points and the Gaussian quadrature method yields the lowest error. The error in the Gaussian quadrature method remains on the order of 10^{-15} except at values of N below 10 while the error in both the trapezoid and Simpson's rules decreases with N .

$$\epsilon_N = I_{2N} - I_N \quad (2)$$

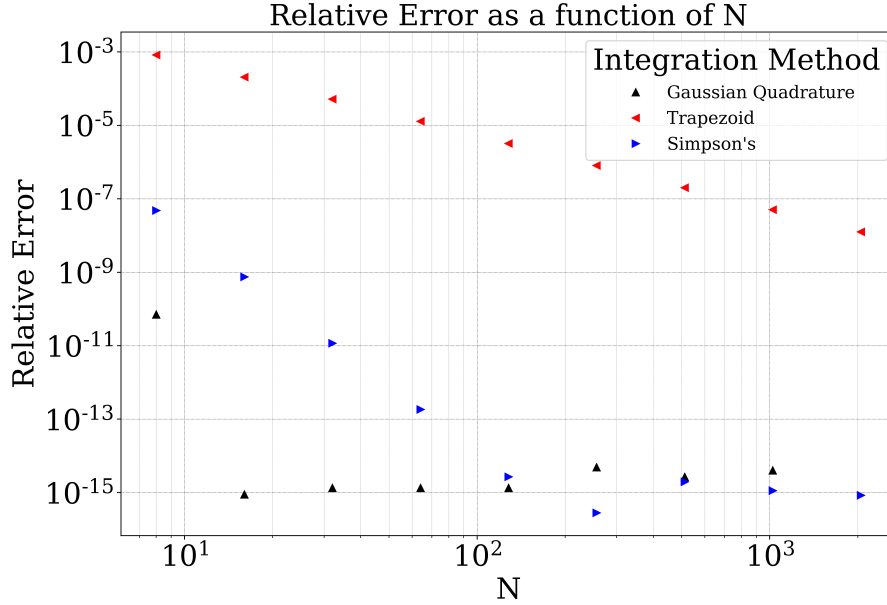


Figure 1: Relative error of the three integration methods for computing the integral given by Eq. 1 as a function of the number of slices/sample points. Both the x and y axis are plotted in a log scale.

1.b Diffraction of Sound Waves

1.b.1

We then calculated the intensity of a wave that is diffracted by being blocked by an object with a straight edge. This intensity is given by Eq. 3 where $C(u)$ and $S(u)$ are the Fresnel integrals given by equations 4 and 5 where u is defined in 6. In these equations I_0 is the intensity of the wave before diffraction, λ is the wavelength and x and z are the position coordinates past the straight edge.

$$I = \frac{I_0}{8} ([2C(u) + 1]^2 + [2S(u) + 2]^2) \quad (3)$$

$$C(u) = \int_0^u \cos\left(\frac{1}{2}\pi t^2\right) dt \quad (4)$$

$$S(u) = \int_0^u \sin\left(\frac{1}{2}\pi t^2\right) dt \quad (5)$$

$$u = z\sqrt{\frac{2}{\lambda z}} \quad (6)$$

To do this we set $\lambda = 1\text{m}$, $z = 3\text{m}$, and x to be an array of 100 values between -5m and 5m . Then, we used the Gaussian quadrature method to numerically evaluate the Fresnel integrals in the intensity equation with $N = 50$ sample points and then computed (I/I_0) . We then computed this same intensity using `scipy` to evaluate the Fresnel integrals. These two sets of intensity values were then plotted as a function of x and can be seen in Fig. 2. This plot shows that the two solutions are equivalent, indicating that the Gaussian quadrature method correctly evaluated the integrals.

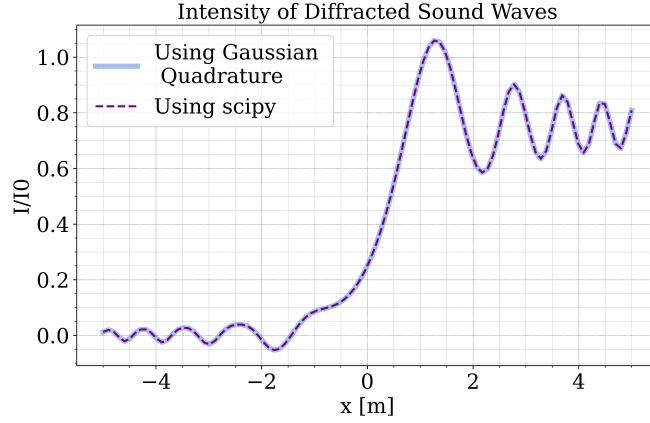


Figure 2: The intensity of diffracted sound waves as a function of x obtained from equation 3. The Gaussian quadrature method (blue line) and the `scipy` (purple dotted line) solution of the Fresnel integrals yield almost identical results.

We then plotted the relative difference between the two methods (Gaussian quadrature and `scipy`) using Eq. 7. These differences were then plotted as a function of x and can be seen in Fig. 8.

$$\delta(x) = \frac{|I_{SP} - I_G|}{I_{SP}} \quad (7)$$

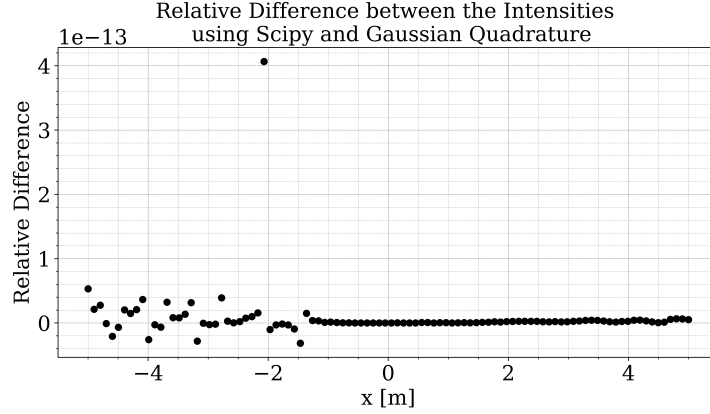


Figure 3: The relative difference between the Gaussian quadrature method and the `scipy` solution to Eq. 3. The relative difference is computed as in Eq. 7.

1.b.2

We then repeated this calculation of the intensity using Gaussian quadrature with a range of N values varying from 3 to 50 and computed the maximum relative difference between each of these computations with the value obtained using `scipy`. As can be seen in Fig. 3, there is one point near $x = -2\text{m}$ where the relative difference is significantly larger than all of the other relative difference points. There is a point like this for each value of N , and this is because at this point we are dividing by small values. To account for this, we took the maximum of the relative difference values only where $x > 0$ so as not to include this point. These values were then plotted as a function of N and can be seen in Fig. 4. This plot shows that the relative error is large for values of N below $N = 10$ but at $N = 10$ this maximum error approaches zero. This indicates that 50 samples were not needed but that 10 would have been sufficient.

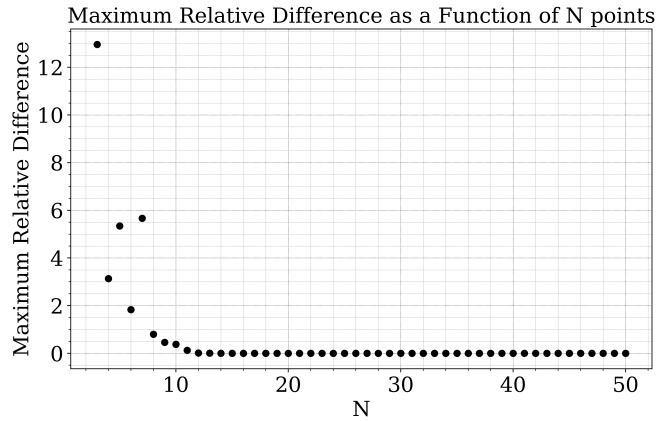


Figure 4: The maximum relative difference between the Gaussian quadrature method and the `scipy` solution to Eq. 3 for a range of N sample numbers from 3 to 50. This maximum difference was taken in the range of intensity values corresponding to the domain of $x > 0$.

1.c

We then created two dimensional contour plots of the intensity computed with the Gaussian quadrature method with a range of x values from -3m to 10m and a range of z values from 1m to 5m. Figures 5a, 5b and 5c depict these contour plots with wavelength values of 1m, 2m and 4m respectively. These figures show the diffraction pattern for the intensity of the sound waves. They show that as the wavelength increases, the diffracted sound waves blur and spread out and the intensity decreases slightly. The increase in wavelength causes an increase in diffraction of the sound waves.

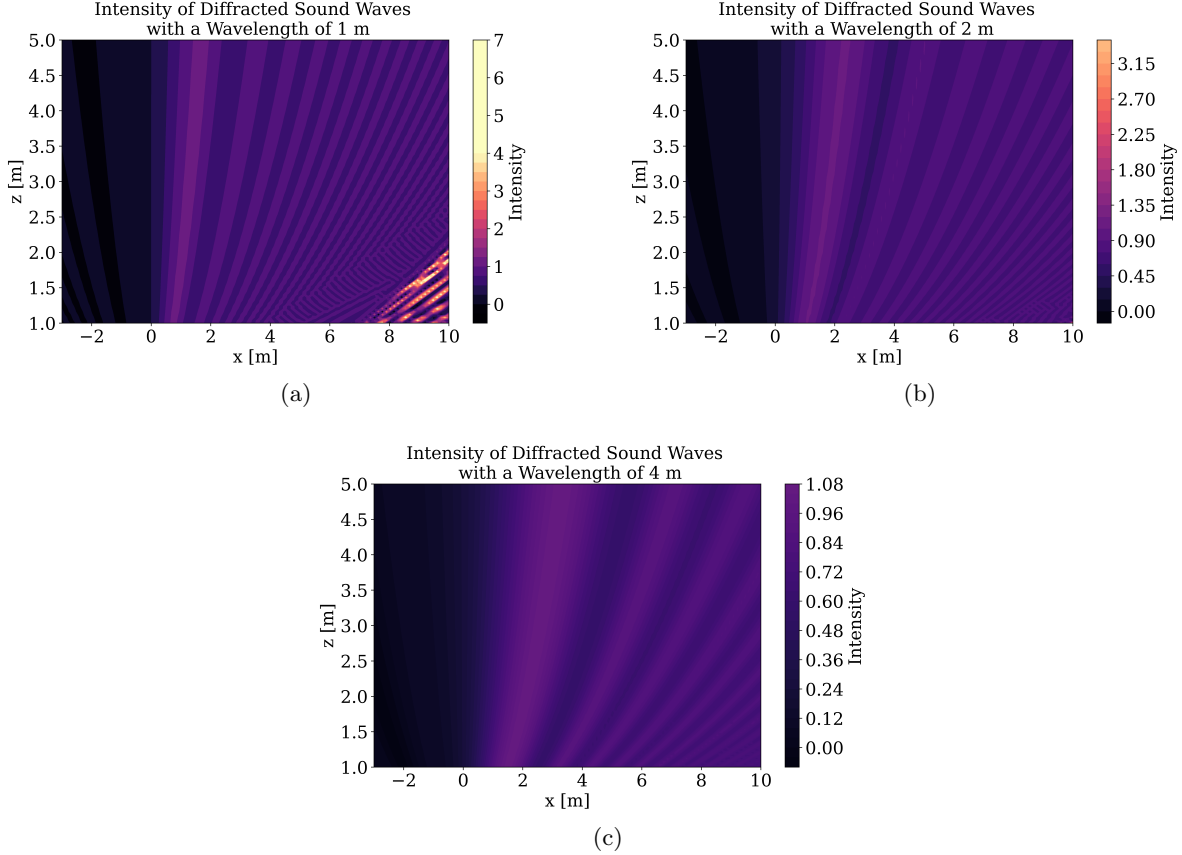


Figure 5: Figure (a) depicts the intensity for diffracted sound waves as computed with the Gaussian quadrature method for waves with a wavelength of 1m. Figure (b) depicts the intensity for diffracted sound waves as computed with the Gaussian quadrature method for waves with a wavelength of 2m. Figure (c) depicts the intensity for diffracted sound waves as computed with the Gaussian quadrature method for waves with a wavelength of 4m.

2 The Period of a Relativistic Particle on a Spring

2.a

We confirm that an initial position of $x_0 = 1$ cm corresponds to the classical limit by comparing the potential energy, $\frac{1}{2}k\Delta x^2$, and kinetic energy, mc^2 , of the particle. For a spring constant $k=12$ N/m, mass $m=1$ kg, and $\Delta x = 1$ cm, the ratio of potential to kinetic energy is on the order of -21. Thus Eq. 8 holds and $x_0=1$ cm corresponds to the classical limit.

$$\frac{1}{2}k(x_0^2 - x^2) \ll mc^2 \quad (8)$$

| N | Numerical Value [s] | Fractional Error |
|----|---------------------|------------------|
| 8 | 1.73 | 0.023 |
| 16 | 1.77 | 0.012 |

Table 2: Numerical values and fractional errors for the period of a particle on a spring, computed with Gaussian quadrature for N=8 and N=16. The estimated fractional errors were calculated as $\epsilon_{N,frac} = \frac{\epsilon_N}{I_N}$, with the error estimated as Eq. 2

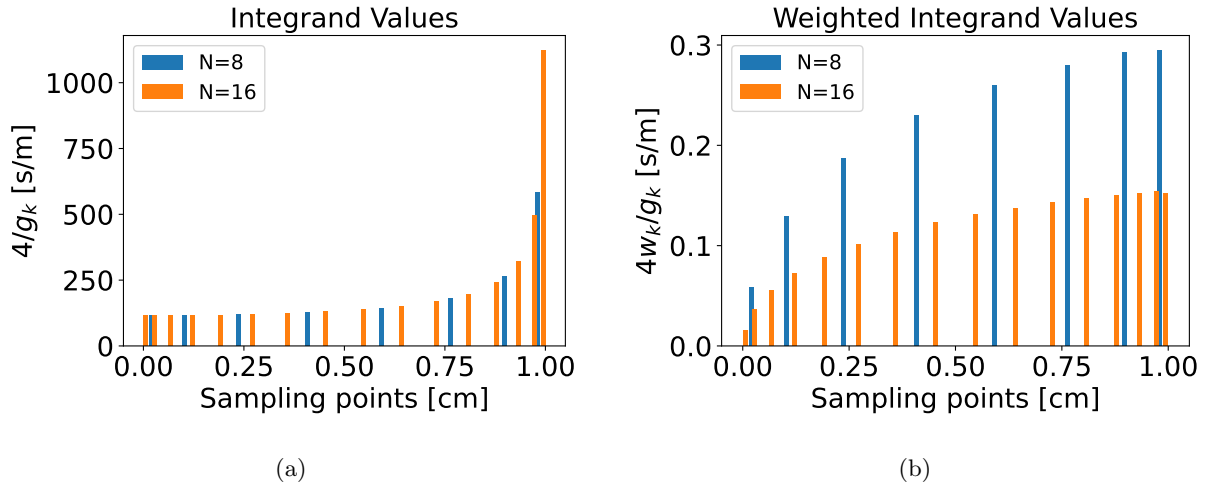


Figure 6: Figure (a) shows the integrand value ($4/g_k$) while Figure (b) shows the weighted integrand value ($4w_k/g_k$) at sampling points for N=8 and N=16.

The integrand values for both the N=8 and N=16 cases rise steeply as x approaches 1cm. This diverging integral results in a lower accuracy for a given number of sampling points. In contrast, the weighted integrand values converge as the sampling point approaches x_0 . Since the value of the integrand changes rapidly as it diverges, we require a large number of sampling points as x approaches 1 cm to increase the accuracy. With more points near the edges than in the centre of the x range, Gaussian quadrature places smaller weights on the sample points near the edge.

2.b

We calculated the initial displacement, $x_0 = x_c > 0$, such that a classical particle on a spring initially at rest would lead to a speed of c at $x = 0$.

The solution to the differential equation (Eq. 9) for the motion of a classical particle on a string is given by Eq. 10.

$$m \frac{d^2 x}{dt^2} = -kx \quad (9)$$

$$x(t) = e^{\pm i \sqrt{\frac{k}{m}} t} \quad (10)$$

We plug Eq. 10 into the right hand side of Eq. 9 and integrate both sides from t_0 to $t|_{x=0, v=c}$.

$$c = \int_{t_0}^{t|_{x=0, v=c}} \frac{d^2x}{dt^2} dt = -\frac{k}{m} \int_{t_0}^{t|_{x=0, v=c}} e^{\pm i\sqrt{\frac{k}{m}}t} dt \quad (11)$$

$$c = -\frac{k}{m} [\mp i\sqrt{\frac{m}{k}} e^{\pm i\sqrt{\frac{k}{m}}t}]_{t_0}^{t|_{x=0}} = \pm\sqrt{\frac{k}{m}} [x]_{t_0}^{t|_{x=0}} \quad (12)$$

$$x_0 = \pm c\sqrt{\frac{m}{k}} \quad (13)$$

Since we defined $x_c > 0$, the initial displacement that satisfies the conditions of Q2b is $x_0 = +c\sqrt{\frac{m}{k}}$. So for $m = 1\text{kg}$ and $k = 12\text{N/m}$, as given in Q2, we calculate $x_0 = \frac{1}{2\sqrt{3}}c$.

2.c

The period computed with Gaussian quadrature for $N=200$ was 1.81025s with a percentage error of 0.098%. The estimated percentage error was calculated as $\epsilon_{N, pct} = \frac{\epsilon_N}{I_N} \times 100\%$, with the error estimated as Eq. 2.

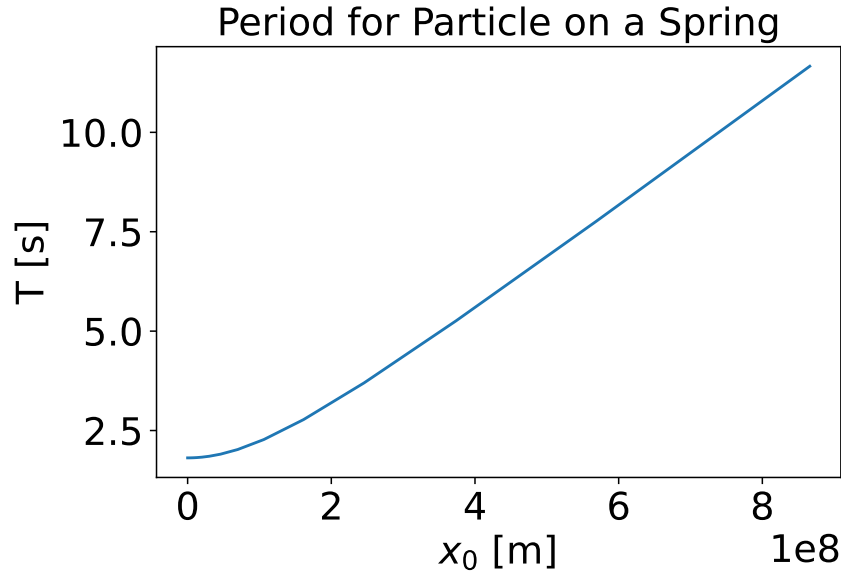


Figure 7: The period of a particle on a spring initially at rest, for a range of initial positions, x_0 from $1m < x < x_c = \frac{1}{2\sqrt{3}}c$. The integral was computed with Gaussian quadrature for $N=200$. The small x_0 shows the classical limit, while large x_0 shows the relativistic limit.

Figure 7 shows that the period is practically independent of its initial position when x_0 is sufficiently small. This agrees with the classical limit of $T = 2\pi\sqrt{\frac{m}{k}}$, which has no x_0 term. For sufficiently large x_0 , Figure 7 shows that the period increases linearly. This agrees with the relativistic limit of $T = 4x_0/c$, which is proportional to x_0 .

3 Numerical Differentiation Errors

3.a

$$f(x) = e^{-x^2} \quad (14)$$

The numerical value for the derivative of Eq. 14 at $x = 0.5$ was computed using the forward difference scheme (Eq. 15) for various step sizes, h , ranging from 10^{-16} to 10^0 . The results are shown in Figure 3.

$$\frac{df}{dx} = \frac{f(x+h) - f(x)}{h} \quad (15)$$

3.b

$$\frac{d}{dx}e^{-x^2} = -2xe^{-x^2} \quad (16)$$

The analytic value of Eq. 14 at $x = 0.5$ is $-e^{-0.25}$. The absolute value of the error was computed by comparing the analytic value of 14 with the numerical value found in Section 3.a for each h .

| $\log(h)$ | Numerical Value (Q3a) | Error (absolute value) |
|-----------|-----------------------|------------------------|
| -16 | -1.11e+00 | 3.31e-01 |
| -15 | -7.77e-01 | 1.64e-03 |
| -14 | -7.77e-01 | 1.64e-03 |
| -13 | -7.79e-01 | 5.76e-04 |
| -12 | -7.79e-01 | 2.07e-05 |
| -11 | -7.79e-01 | 1.54e-06 |
| -10 | -7.79e-01 | 6.85e-07 |
| -9 | -7.79e-01 | 1.86e-08 |
| -8 | -7.79e-01 | 7.45e-09 |
| -7 | -7.79e-01 | 3.85e-08 |
| -6 | -7.79e-01 | 3.89e-07 |
| -5 | -7.79e-01 | 3.89e-06 |
| -4 | -7.79e-01 | 3.89e-05 |
| -3 | -7.79e-01 | 3.89e-04 |
| -2 | -7.83e-01 | 3.83e-03 |
| -1 | -8.11e-01 | 3.24e-02 |
| 0 | -6.73e-01 | 1.05e-01 |

Table 3: Numerical values and absolute errors of the derivative of Eq. 14 using the forward difference scheme for various step sizes, h , ranging from 10^{-16} to 10^0 .

3.c

It is clear from Figure 8 that the minimum absolute error for the forward difference scheme occurred at a step size of $h = 10^{-8}$.

$$\epsilon = \frac{2C|f(x)|}{h} + \frac{1}{2}h|f''(x)| \quad (17)$$

The total error for the forward difference scheme (Eq. 17) consists of 2 components - the rounding error (first term) and approximation error (second term). The rounding error increases proportionally to $\frac{1}{h}$ while the approximation error decreases proportionally to h as h approaches zero. The

curve of the forward difference scheme errors shown in Figure 8 depends on the balance between these two terms. The total error increases while the rounding term increases faster than the approximation term decreases, and it decreases while the approximation term decreases faster than the rounding term increases. We can show that the curve should be at a minimum at $h = 10^{-8}$, as shown in Figure 8, by finding the root of the derivative of ϵ and applying the second derivative test.

$$0 = \frac{d\epsilon}{dh} = -\frac{2C|f(x)|}{h^2} + \frac{1}{2}|f''(x)| \quad (18)$$

$$h = \sqrt{4C \left| \frac{f(x)}{f''(x)} \right|}$$

So for $f(0.5) = f''(0.5) = -e^{-0.25}$ and a typical error constant of $C = 10^{-16}$ for Python, the smallest total error is given by a step size of order 10^{-8} .

$$\begin{aligned} \frac{1}{2}h|f''(x)| &> \frac{2C|f(x)|}{h} \\ h &> \sqrt{4C \left| \frac{f(x)}{f''(x)} \right|} \end{aligned} \quad (19)$$

In Eq. 19 we compare the rounding and approximation errors to find that the approximation, or truncation, error dominates for $h > \sqrt{4C \left| \frac{f(x)}{f''(x)} \right|} = 2 \times 10^{-8}$ while the rounding error dominates for $h < \sqrt{4C \left| \frac{f(x)}{f''(x)} \right|} = 2 \times 10^{-8}$.

3.d

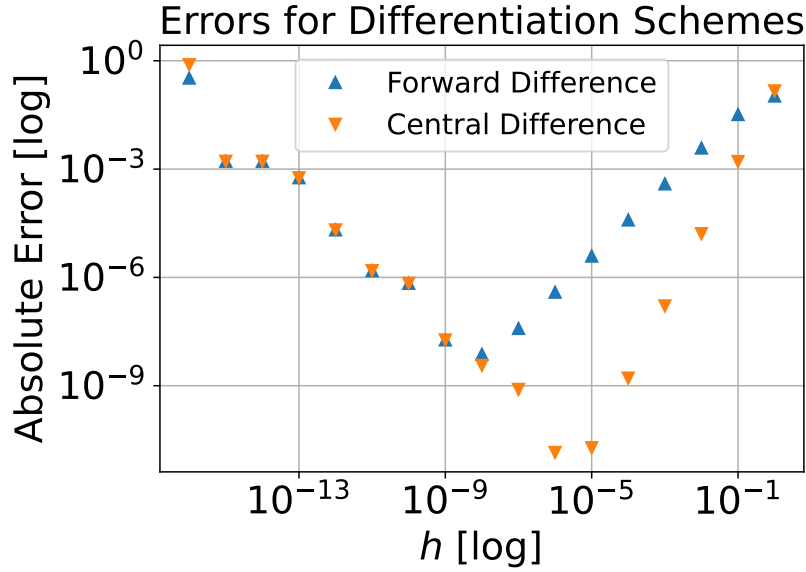


Figure 8: Absolute errors on the numerical value of the derivative of Eq. 14 for varying step size h , using the forward and central difference schemes.

The minimum absolute error for the forward and central difference schemes were 10^{-8} and 10^{-6} , respectively. On either side of the minimum, the error decreased/increased nearly logarithmically. The errors for the two differentiation schemes were very similar up to a step size of 10^{-8} , after which the error for the forward difference scheme increased while the error for the central difference scheme continued to decrease until its minimum at 10^{-6} . At $h = 10^0$, the two errors returned to having approximately the same value. The central difference scheme achieves a minimum error of 10^{-11} ; 2 orders smaller than that of the forward difference scheme.

Figure 8 shows that the 2 schemes have very similar errors for $10^{-15} < h < 10^{-9}$. For $h = 10^{-16}$ and $h = 10^0$ the central difference scheme actually has a larger error than the forward difference scheme. Thus the central difference scheme does not always clearly beat the forward difference scheme in terms of accuracy.